Superalloys 2012: 12th International Symposium on Superalloys
Edited by: Eric S. Huron, Roger C. Reed, Mark C. Hardy, Michael J. Mills, Rick E. Montero, Pedro D. Portella, Jack Telesman
TMS (The Minerals, Metals & Materials Society), 2012

DEVELOPMENT OF A NEW 760°C (1400°F) CAPABLE LOW THERMAL EXPANSION ALLOY

M. Fahrmann, S. K. Srivastava, L. M. Pike
HAYNES International, 1020 West Park Avenue, Kokomo, Indiana, 4690-9013, USA

Keywords: alloy development, age-hardening, thermal expansion, strength, thermal stability

Abstract

A recently developed 760°C (1400°F) capable low thermal expansion alloy, HAYNES® 244™ alloy, is introduced. The new alloy is intended for use in seal rings and other static parts of future generation gas turbines operating at higher temperatures. The alloy is an improvement over current generation low thermal expansion alloy HAYNES 242® alloy. Its defining feature is the partial substitution of tungsten for molybdenum. Judicious alloying enabled the same age-hardening mechanism to be operative while increasing the thermal stability of the strengthening phase, thus raising the temperature capability of the new alloy. The results of a mill scale-up of this concept are reported with regard to several key performance characteristics: thermal expansion, tensile and creep strength, and thermal stability. While additional product forms such as plate and sheet are being processed, the bulk of the presented results relates to capability pancakes obtained from forged billet. Benchmarking against several current generation low thermal expansion alloys indicates the potential of the new alloy for more demanding operating conditions.

Introduction

The demand for more fuel efficient gas turbines drives the need for higher operating temperatures, thus impacting material requirements for both rotating and static parts. In the latter category, current generation low thermal expansion alloys such as HAYNES 242 alloy or INCONEL® alloy 783 appear to be limited to service temperatures of approximately 649°C (1200°F).

Addressing the need for a higher temperature capable, yet low thermal expansion alloy, HAYNES 244 alloy has been developed [1]. This new alloy builds conceptually on the metallurgy of HAYNES 242 alloy (nominal composition Ni – 8 Cr - 25 Mo) : imparting strength by the formation of ordered domains upon age hardening, and ensuring low thermal expansion by virtue of a high refractory element content [2]. On a lab scale it was found that particularly tungsten, when replacing a portion of the molybdenum, resulted in higher temperature capable material. Hence, the new alloy's nominal composition (in weight percent) was selected to be Ni – 8 Cr – 22.5 Mo – 6 W, with nickel being the balance and carbon as low as possible.

The purpose of this paper is (a) to report key material properties obtained with a first mill-scale heat of this new alloy, and (b) to elucidate the beneficial role of tungsten. The material properties are benchmarked against those of several commercial current generation low thermal expansion alloys.

Scale-Up

Mill-Scale Heat

A mill-scale heat was melted to the aforementioned aim, and cast into two electrodes, both of which were electro-slag re-melted into 406 mm (16") diameter ingots. Melt and re-melt practices were similar to those employed in the production of 242 alloy.

After a homogenization treatment, ingot 1 was press forged to 200 mm (8") and 162 mm (6.5") diameter billet stock, respectively. Several slices were cut from these billets, macro-etched, and examined to ASTM E-340. No macro-segregation was found.

Slugs were obtained from the center of the billets, and up-set forged at 1121°C (2050°F) to approximately 18 mm (¾") thick pancakes. The corresponding reduction was 4.3 : 1 in all instances.

Blanks, which were extracted from these pancake forgings, provided the bulk of the sample stock for subsequent heat treating, testing, and characterization. Care was exercised that areas affected by the die lock in the course of pancake forging were excluded from testing and evaluation.

A portion of ingot 2 was recently forged to a slab, and subsequently hot rolled to 12.5 mm (½") thick plate. Transverse tensile blanks obtained from this plate provided the basis for some, albeit presently limited, comparative testing of different product forms.

Heat Treatment and Microstructure

The solution annealing parameters were optimized to 1135°C (2075°F) / 30 min / water quench by balancing strength, ductility (containment factor), and grain size. In this condition, the grains were equiaxed and their distribution normal as shown in Fig. 1. The average grain size was read to ASTM no. 4. Some light grain banding, associated with stringers of un-solutioned primary precipitates, is discernable. The nature of these primary precipitates will be discussed in the physical metallurgy section.

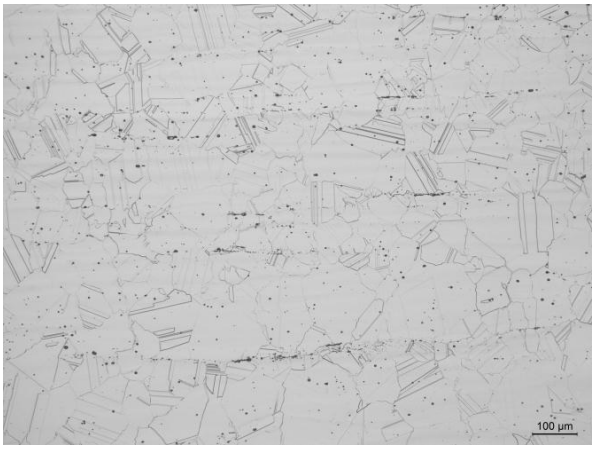

Figure 1. Light microscopy micrograph of the typical grain structure of 244 alloy pancake blanks in the solution-annealed condition.

For age-hardening, the same two-step aging cycle devised for the lab scale heats was adopted : 760°C (1400°F) / 16 h / furnace cool to 649°C (1200°F) / 32 h / air cool. As a result of this aging treatment, sub-micron size distinct precipitates (their long axis being on the order of 500 nm) formed as shown in Fig. 2. Their morphology is presumably lenticular, and several orientational variants are apparent. Notice that these features nucleated homogeneously in the bulk of the grains. No denuded zones along grain or twin boundaries were apparent. Due to their similar morphology compared to the features found in aged 242 alloy [2], these precipitates will be referred to as "domains".

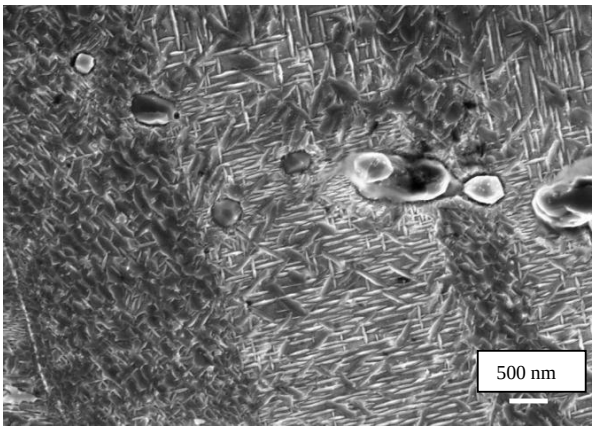

Figure 2. SEM in-lens image of the typical domain structure in 244 alloy pancake blanks in the annealed plus aged condition.

Strength

Tensile Strength

Tensile bars were machined from fully heat treated pancake blanks, and tested at room and elevated temperatures in accordance with ASTM standards E-8 and E-21, respectively. To elucidate the impact of the two-step aging treatment, several as-solution annealed blanks were also tested at selected temperatures. The data, along with comparative strength data for fully heat treated 242 alloy bars and rings [3], is compiled in Table I.

Table I. Representative room and elevated temperature tensile data of heat treated 242 alloy and 244 alloy product forms.

alloy	**test T**	**Y.S.**	**U.T.S.**	**EL**	**RA**
	[°C]	[MPa]	[MPa]	[%]	[%]
242	RT	844	1292	34	45
bar & ring	94	761	1246	32	47
ann. + aged	205	705	1196	33	51
	316	665	1162	33	48
	427	595	1112	38	45
	538	540	1078	38	49
	649	570	999	33	41
	760	309	732	44	54
	872	308	500	50	85
	983	211	289	54	97
244	RT	396	903	67	72
pancake	649	274	754	73	57
annealed	760	272	708	67	47
	872	260	493	78	63
244	RT	848	1365	35	40
pancake	427	707	1179	44	49
ann. + aged	538	686	1116	41	52
	649	649	996	25	31
	649*	653	1009	36	52
	760	479	731	46	44
	760*	450	783	53	47
	872	252	377	146	86
244	RT	847	1333	35	39
plate	649	634	1002	30	29
ann.+ aged	760	459	719	53	44

* 10x the standard cross-head speed from yield point to fracture

The respective strength data is plotted in Fig. 3.

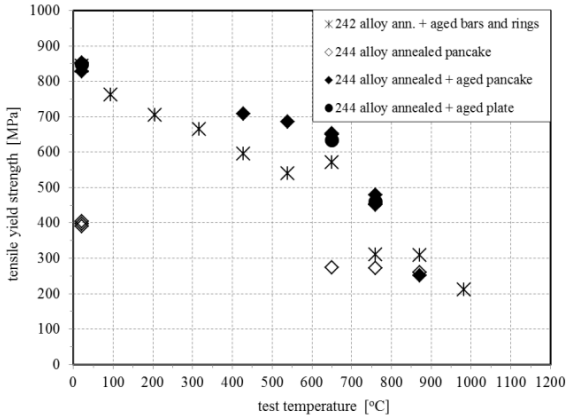

Figure 3. Plot of comparative yield strength data of 242 alloy (benchmark) and of the new 244 alloy as a function of test temperature.

Several important conclusions may be drawn from this plot : (a) upon the devised two-step aging treatment, the strength of 244 alloy roughly doubled, and (b) the new 244 alloy has a distinct strength advantage over 242 alloy at 760°C (1400°F), at least for the product forms evaluated.

As for the age hardening effect, it is noted that the new alloy rapidly softens at higher temperatures : some hardness is still retained after exposures to 774°C (1425°F), however, an one hour exposure to 788°C (1450°F) completely eradicated the hardening effect.

Tensile Ductility

Low thermal expansion alloys are known to be susceptible to embrittlement in oxygen-containing environments by virtue of their low chromium contents [4]. One measure of this susceptibility is the alloy's elevated temperature tensile elongation, particularly at 649°C (1200°F). In Fig. 4, this data corresponding to the strength data in Fig. 3 is plotted.

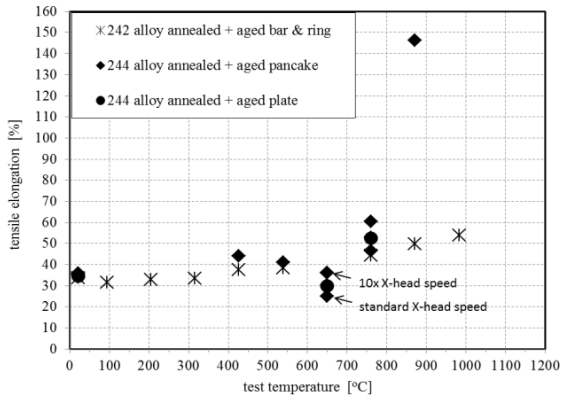

Figure 4. Plot of tensile elongation of 242 and 244 alloys as a function of test temperature.

The data exhibits a decrease in elongation at 649°C (1200°F). However, the ductility debit depends on strain rate as indicated by the arrows: higher strain rates tend to suppress embrittlement in the course of straining, hence, a larger elongation at failure. Similar trends have been reported for HAYNES 242 alloy [5]. Tensile elongations of greater than 20 % even at the relatively low standard cross-head speeds are quite encouraging.

Creep Rupture Strength

Smooth and combination creep rupture bars were machined from fully heat treated pancake blanks, and tested at temperatures ranging from 649°C (1200°F) to 760°C (1400°F) in accordance with ASTM standards E-139 and E-292, respectively.

None of the tests failed in the notch. A log stress – log 1% creep life plot of the data is shown in Fig. 5. The straight lines, test temperature being the parameter, were regressed using a power law.

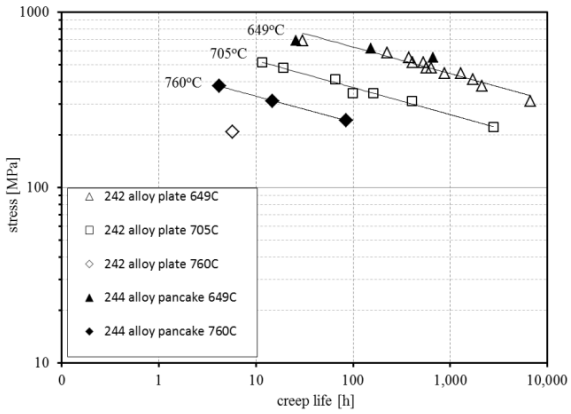

Figure 5. Log stress – log 1% creep life plot of creep data of 242 alloy and new 244 alloy.

The greater creep strength of 244 alloy over 242 alloy at 760°C (1400°F) is evident. At temperatures of 705°C (1300°F) or less, it appears that the creep strengths of the two alloys are comparable as suggested by the Larson-Miller plot in Fig. 6. However, more testing of 244 alloy in this temperature range (particularly in plate product form) will be required to substantiate this statement.

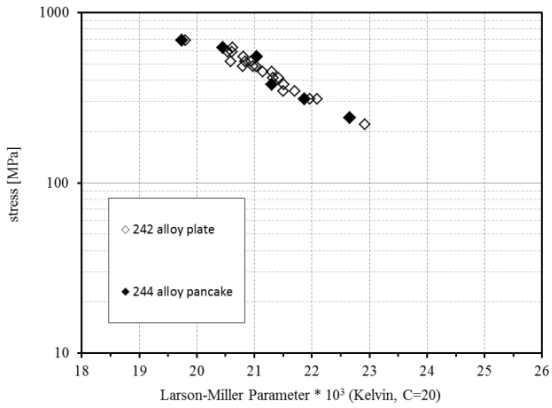

Figure 6. Larson-Millet plot of 1 % creep lives of 242 alloy (at temperatures of 706°C (1300°F) or less) and new 244 alloy.

The new alloy's higher temperature capability is also reflected in the creep-rupture lives plotted in Fig. 7. In fact, 244 alloy even meets the 760°C (1400°F) / 310 MPa (45 ksi) rupture life of alloy 718 of approximately 100 hours [3].

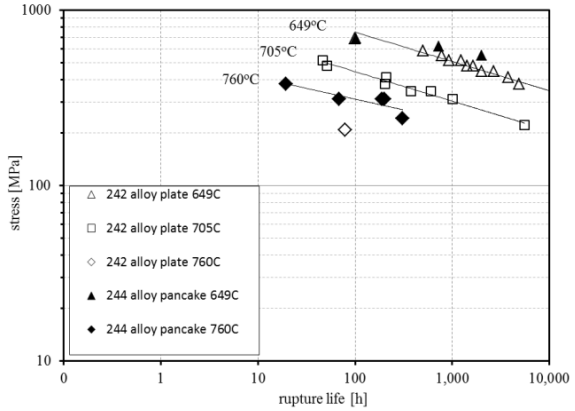

Figure 7. Log stress - log rupture life plot of 242 alloy and new 244 alloy.

Thermal Expansion

Thermal expansion measurements were conducted on carefully machined and low-stress-ground pins in accordance with ASTM E228. Figure 8 shows the mean coefficient of thermal expansion (CTE) between room temperature and the indicated test temperature for 244 alloy and several current-generation low CTE alloys.

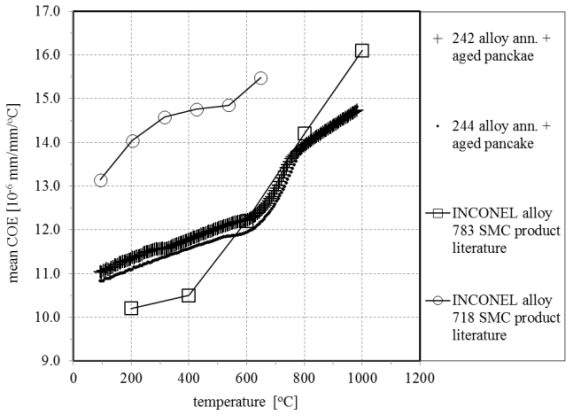

Figure 8. Mean coefficient of thermal expansion of new 244 alloy and several current generation low CTE alloys.

Notably, 244 alloy exhibits the lowest mean CTE of any of these alloys when tested in excess of 538°C (1000°F). Interestingly, its CTE exhibits an inflection point at approximately 788°C (1450°F), which coincides with the alloy's softening temperature. HAYNES 242 alloy displays a similar behavior, however, with an inflection point shifted to lower temperatures.

Thermal Stability

Sufficient thermal stability is one of the key performance criteria for any high-temperature alloy. In order to assess the potential for degradation in microstructure and properties, fully heat treated pancake blanks were thermally exposed for 1,000 hours to temperatures of 649 / 705 / 760°C (1200 / 1300 / 1400°F).

Microstructure Evolution

High-resolution SEM in-lens images of the over-aged microstructures are shown in Figs. 9 – 11.

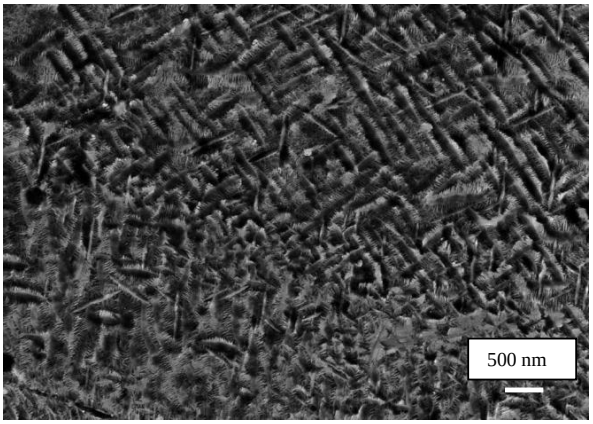

Figure 9. SEM in-lens image of the typical microstructure of 244 alloy after a 649°C (1200°F) / 1,000 h thermal exposure.

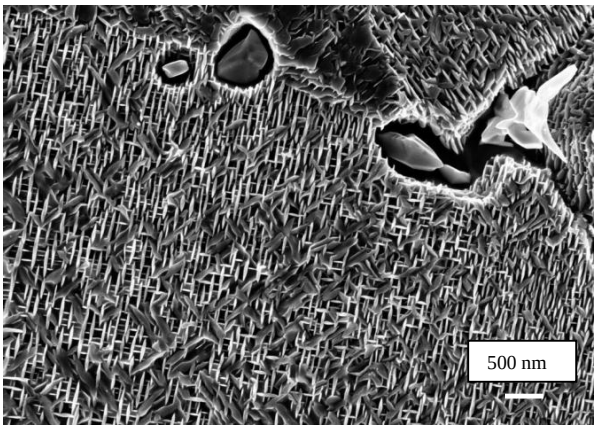

Figure 10. SEM in-lens image of the typical microstructure of 244 alloy after a 705°C (1300°F) / 1,000 h thermal exposure.

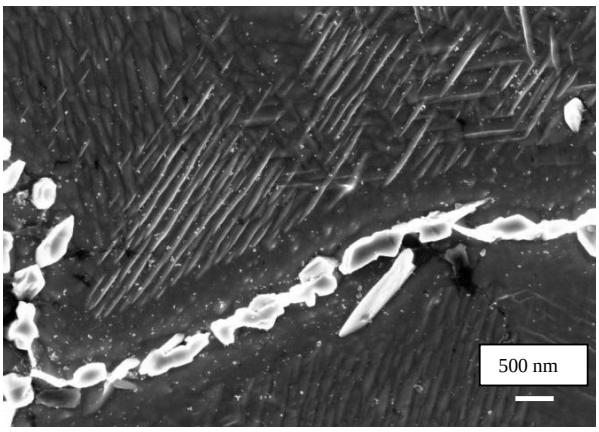

Figure 11. SEM in-lens image of the typical microstructure of 244 alloy after a 760°C (1400°F) / 1,000 h thermal exposure.

The microstructure in Fig. 9 clearly displays a bi-modal domain size distribution, which was not apparent in the as-heat treated condition (see Figure 2). The characteristic dimensions of the coarser (primary) domains are comparable to those in the as-heat treated condition. In contrast, the finer second domain population must have formed upon the extended thermal exposure, indicative of a residual supersaturation of solute elements in the as-heat treated condition.

Such fine, secondary domains were not discernable after long-term aging at 705°C (1300°F) (Fig. 10). Coarsening of the primary domains appeared to be minor.

The defining features of the 760°C (1400°F) exposed condition were (a) coarsened primary domains, and (b) inter- and intra-granular Mo- and W-rich bulky particles (as verified by SEM / EDS). The latter were consistently associated with domain-denuded zones. Hence, the conjecture of a gradual dissolution of the domains and their transformation into a more stable phase(s).

Retained Tensile Properties

Retained tensile properties after the aforementioned thermal exposures are displayed in Fig. 12 (tested at room temperature) and Fig. 13 (tested at 760°C (1400°F), respectively.

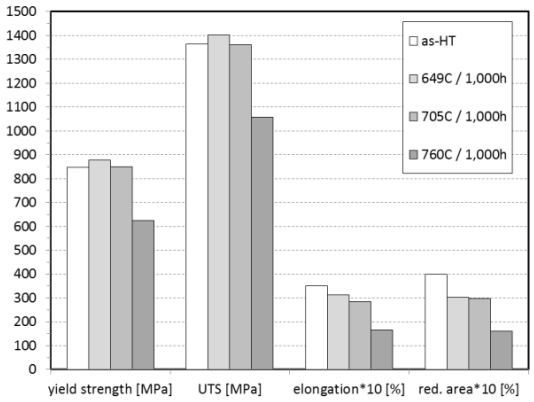

Figure 12. Retained room temperatures tensile properties of the new 244 alloy after various thermal exposures.

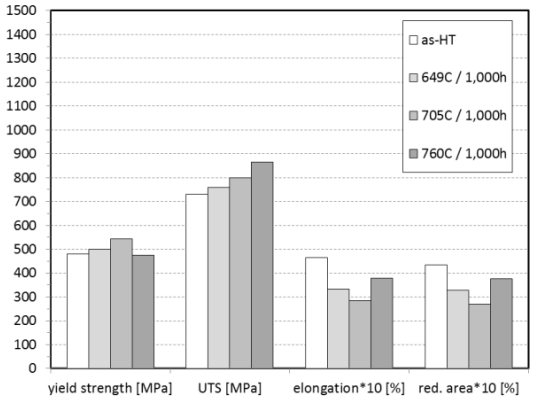

Figure 13. Retained 760°C (1400°F) tensile properties of the new 244 alloy after various thermal exposures.

Consistent with the preceding discussion about the secondary domains, the material continued to age-harden upon extended exposure to 649°C (1200°F) (the lower aging temperature). Extended exposure to 760°C (1400°F) (the higher aging temperature) resulted in some debit in strength and ductility, presumably due to the gradual transformation taking place in the material. However, application-relevant elevated temperature strength characteristics were still comparable to those in the as-heat treated condition.

Physical Metallurgy

Solidification and Segregation

The light grain banding discernable in Fig. 1 was associated with stringers of coarse primary precipitates, which could not be solution annealed. SEM / EDS work verified their enrichment in Mo and W over the matrix. Phase extraction / XRD suggested the predominance of μ (chemical formula $Cr_{20}Mo_{43}Ni_{37}$, hexagonal crystal system) and P (chemical formula $Cr_9Mo_{21}Ni_{20}$, orthorhombic crystal system) phases; M_6C type carbide was

clearly the minority phase [6]. These findings are consistent with the alloys' low carbon content and the strong partitioning of Mo to the inter-dendritic liquid in the course of solidification of the ESR ingot. The latter claim is supported by a Scheil simulation shown in Fig. 14 utilizing the CALPHAD software PANDAT [7] in conjunction with the thermodynamic database Ni-DATA [8].

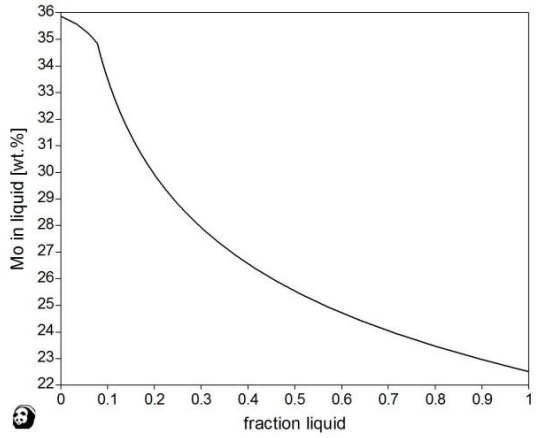

Figure 14. Scheil simulation of the partitioning of Mo to the liquid in the course of solidification of 244 alloy.

Remarkably, W is predicted to exhibit inverse partitioning to Mo, i.e., enrichment in the dendrite cores (Fig. 15).

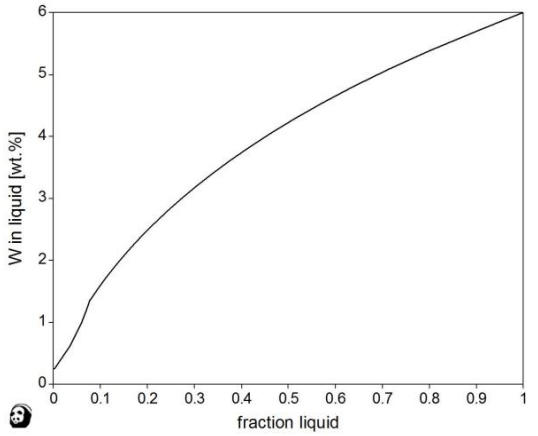

Figure 15. Scheil simulation of the partitioning of W to the liquid in the course of solidification of 244 alloy.

While the initial concentration gradients between dendrite cores and inter-dendritic regions were greatly mitigated in the course of ingot homogenization and thermo-mechanical processing, measured residual micro-segregation patterns supported above notion. To this end, the (homogeneous) matrix composition of properly annealed samples was probed by EDS in the vicinity and away from the primary precipitates. The results are compiled in Table II. Note that these are the extremes of the matrix composition variation.

Table II. Standard-less EDS spot analyses of local matrix compositions (in wt.%, balance Ni) in annealed 244 alloy.

location	probe	Mo	W	Cr
vicinity	spot 1	24.35	6.95	7.47
"	spot 2	24.76	7.39	7.84
"	spot 3	23.94	7.43	7.88
	avg.	**24.35**	**7.26**	**7.73**
away	spot 4	21.44	8.72	7.81
"	spot 5	21.48	8.70	7.74
"	spot 6	21.61	8.61	7.76
	avg.	**21.51**	**8.68**	**7.77**

Chromium, as predicted, did not exhibit any significant concentration gradient. The opposite partitioning behaviors of Mo and W would, in theory, help to render the alloy less prone to macro-segregation by diminishing the density inversion factor [9].

Age Hardening

Upon the devised two-step age-hardening treatment, 244 alloy formed (presumably lenticular) precipitates ("domains") as shown in Fig. 2. In order to elucidate their crystal structure, thin foils were prepared by twin-jet polishing in a solution of 1 part nitric acid and 3 parts methanol. The bath temperature was – 40°C, and a potential of 6 V was applied. These thin foils were examined in a TEM operating at 200 kV.

Selected area diffraction patterns consistently exhibited superlattice reflections at 1/3 {220} and 1/3 {113} locations in reciprocal space. Examples of <100> and <114> zone axes diffraction patterns are given in Figs. 16 and 17. The fundamental reflections were indexed in terms of the fcc matrix.

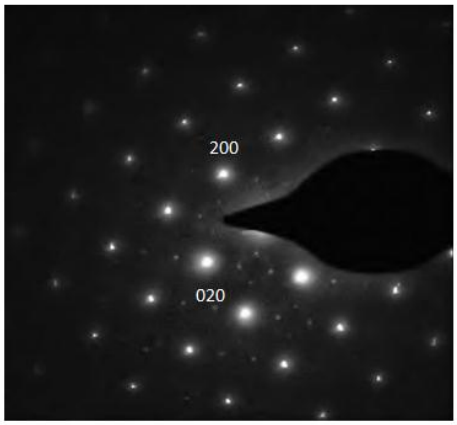

Figure 16. Selected area diffraction pattern of annealed and two-step aged 244 alloy. [001] zone axis.

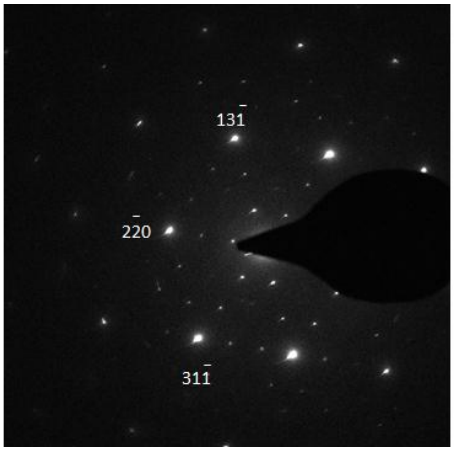

Figure 17. Selected area diffraction pattern of annealed and two-step aged 244 alloy. [114] zone axis.

The location of these superlattice reflections is a characteristic of the $Ni_2(Cr,Mo)$ phase (body-centered orthorhombic lattice, Pt_2Mo structure type), which may form by a special re-arrangement of the solute atoms on the fcc parent lattice [10]. Six orientational variants of this phase exist with respect to the fcc parent lattice, as supported by the various micrographs in this paper.

Hence, partial substitution of W for Mo (at least within the compositional limits of 244 alloy) did not change the nature of the strengthening phase as compared to HAYNES 242 alloy [2].

In order to shed light on the partitioning behavior of W in the course of age hardening, SEM / EDS were performed on selected thin foils. A typical back-scattered electron (BSE) image of areas examined along with the probed locations is shown in Fig. 18. This particular sample was studied in the 760°C (1400°F) / 1,000 hours over-aged condition. As discussed before, its microstructure featured coarsened domains, Mo-and W-rich grain boundary precipitates, and domain-denuded zones.

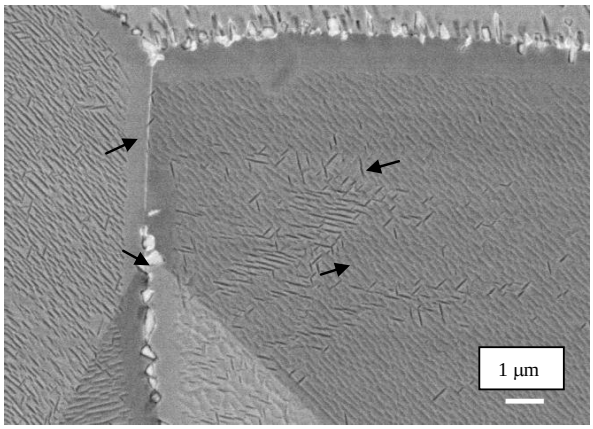

Figure 18. BSE image of the thinned over-aged sample of 244 alloy employed for detailed SEM / EDS work. Probed locations are indicated by arrows.

The results of the local composition analyses were superimposed on a Gibbs triangle (Fig. 19). Superimposed are also corresponding matrix and domain compositions measured on aged HAYNES 242 alloy [11].

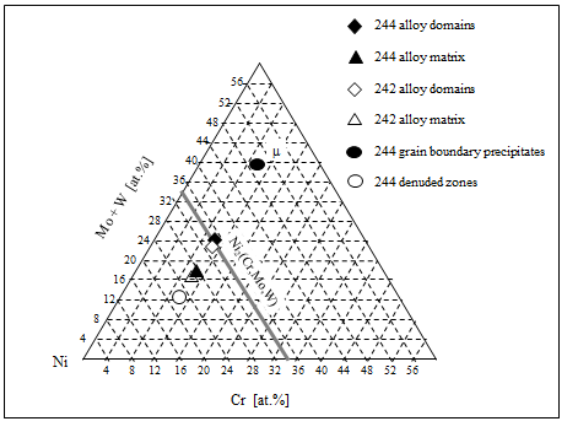

Figure 19. Chemical composition of various constituents in aged 242 and new 244 alloys.

By adding Mo and W on an atomic basis, it becomes apparent that a chemical formula of $Ni_2(Cr,Mo,W)$ is appropriate for the domains. Notice that the matrix adjacent to the domains is diluted in the solutes Mo and W. Hence, it appears that a first-order phase transformation took place in the course of aging.

While no stable Ni_2W phase of Pt_2Mo structure is known to exist in the Ni – W binary system [12], an argument for a metastable quaternary phase can be made. Kinetically the formation of $Ni_2(Cr,Mo,W)$ should be favored over the formation of the Mo / W-rich compound designated μ in Fig. 19 since less solute needs to be re-distributed by diffusion.

The beneficial role of W for the enhanced thermodynamic stability of the $Ni_2(Cr,Mo,W)$ phase over the $Ni_2(Cr,Mo)$ phase is evident from the various high-temperature properties. It is suspected that W increases the enthalpy of formation of the Pt_2Mo type phase as suggested by Fig. 20. Note the significantly greater off-set of the 244 data over the 242 data relative to the corresponding baselines, reflective of a stronger endothermic reaction upon heating (requiring a greater amount of heat to dissolve the ordered domains).

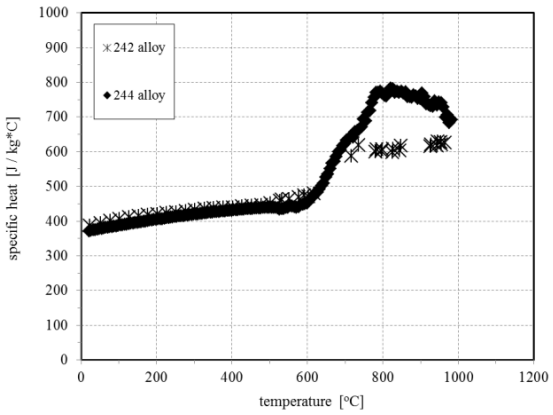

Figure 20. Measured specific heat of fully heat treated 242 alloy and 244 alloy samples as a function of temperature.

As discussed in the section on thermal stability, it appears that the alloy gradually transforms upon extended exposures to 760°C (1400°F) to its final equilibrium phase constitution, presumably γ + μ. The presence of the latter phase was verified by phase extraction / XRD on long-term exposed samples. However, due to the enhanced thermodynamic stability of the $Ni_2(Cr,Mo,W)$ phase, and the known sluggishness of diffusion of W in the fcc matrix relative to Cr and Mo [13], it is expected that the alloy will be thermally sufficiently stable for the intended advanced applications. To this end, long-term exposures going well beyond the reported 1,000 hour results are underway.

Additional important characteristics of the new HAYNES 244 alloy such as formability, weldability, and oxidation resistance, are currently being explored.

Summary and Conclusions

1. HAYNES 244 alloy is a new 760°C (1400°F) capable low-thermal expansion alloy intended for use in static parts of advanced gas turbines.

2. Its nominal composition in weight percent is Ni – 8 Cr – 22.5 Mo – 6 W. A first mill-scale heat was made, and several product forms (billet, plate) have been produced.

3. In the fully heat treated condition, the alloy offers a distinct strength advantage (tensile and creep) over HAYNES 242 alloy. Its mean coefficient of thermal expansion at temperatures exceeding 538°C (1000°F) is lower than that of current generation low-thermal expansion alloys.

4. Detailed characterization suggests that the alloy, like 242 alloy, age-hardens by the formation of $Ni_2(Cr,Mo,W)$ domains of the Pt_2Mo structure type. By alloying this ordered phase with tungsten, its thermodynamic stability was raised over that of $Ni_2(Cr,Mo)$ phase, which strengthens 242 alloy.

5. Preliminary thermal stability data (1,000 hour exposures) indicate the potential for property retention up to 760°C (1400°F).

6. Additional important characteristics of the new HAYNES 244 alloy, such as formability, weldability, and oxidation resistance, are currently being evaluated.

Acknowledgments

The authors would like to thank many individuals in Haynes International's Technology Laboratories and Mill Operations for their efforts in alloy development, characterization, and scale-up.

References

[1] L. M. Pike and S. K. Srivastava, "High-temperature, Low Thermal Expansion Ni-Mo-Cr Alloy", U.S. Patent Application 13/398,996 (17 February 2012).

[2] S. K. Srivastava, "A Low Thermal Expansion, High Strength Ni-Cr-Mo Alloy for Gas Turbines", *International Symposium on Superalloys*, eds. S. D. Antolovich et al., (Warrendale, PA : TMS, 1992), 227-236.

[3] Haynes International website http://www.haynesintl.com, product information.

[4] D. F. Smith and J. S. Smith, "A History of Controlled, Low Thermal Expansion Superalloys", *Physical Metallurgy of Controlled Expansion Invar-Type Alloys*, ed. K. C. Russell and D. F. Smith, 1989, 253-272.

[5] S. D. Antolovich, D. L. Klarstrom, and J. F. Radavich, "The Ductility of HAYNES 242 Alloy as a Function of Temperature, Strain Rate, and Environment", *International Symposium on Superalloys*, eds. T. M. Pollock et al., (Warrendale, PA : TMS, 2000), 609-618.

[6] International Centre of Diffraction Data, Database PDF-4+, 2011.

[7] PANDAT software, version 8.1, CompuTherm LLC, Madison, WI, 2008.

[8] Ni-DATA thermodynamic database, version 8, Thermotech Ltd., Surrey, UK, 2009.

[9] P. Auburtin, T. Wang, S. L. Cockroft, and A. Mitchell, "Freckle Formation and Freckle Criterion in Superalloy Castings", *Metall. Mater. Trans*. 31B (2000) 801-811.

[10] M. Kumar and V. K. Vasedevan, "Ordering Reactions in a Ni-25Mo-8Cr Alloy", *Acta mater*. 44(4) (1996) 1591-1600.

[11] M. F. Rothman, D. L. Klarstrom, M. Dollar, and J. F. Radavich, "Structure / Property Interactions in a Long-Range Order Strengthened Superalloy", *International Symposium on Superalloys*, eds. T. M. Pollock et al., (Warrendale, PA : TMS, 2000), 553-562.

[12] T. B. Massalski et al., *Binary Alloy Phase Diagrams,* (ASM International, 1990), 2882.

[13] R. C. Reed, *The Superalloys, Fundamentals and Applications* (Cambridge University Press, 2006), 63.